

The Use of a Panel Method in the Prediction of External Store Separation

Gerrit J. van den Broek*

National Institute for Aeronautics and Systems Technology, Pretoria, South Africa

A computer program, developed to predict the separation characteristics of external stores after release from the carrier aircraft, is discussed. The aircraft is represented by panel singularity distributions along the line of Woodward's USSAERO code. In order to treat external stores of arbitrary geometry, the store is represented in the same manner. Computer times per trajectory are reduced drastically by employing a flow grid method in combination with approximations regarding the aircraft-store interaction. These approximations are compared with the exact solution. Computations are presented regarding the flowfield below a carrier aircraft and the aerodynamic loads on an external store close to the aircraft. Store separation predictions are presented also. The agreement with experimental data is satisfactory and the store separation predictions compare favorably with those obtained with the Nielsen-Goodwin-Dillenius separation computer code.

Nomenclature

a_{ij}	= aerodynamic influence coefficient
c	= local wing chord, Fig. 2
C_L, C_Y, C_N	= lift, side force, and normal force coefficients, respectively
C_m, C_n	= pitching and yawing moment coefficients, respectively
d_s	= store diameter
I_{approx}	= approximation parameter
M_∞	= flight Mach number; freestream Mach number
s	= aircraft wing semispan, Fig. 2
t	= time after release of store
x, y, z	= aircraft coordinate system, Fig. 2
x_c	= wing section coordinate axis, Fig. 2
$\Delta y_s, \Delta z_s$	= distance of store from carriage position
α	= aircraft angle of attack
α_i, β_i	= flow angularities, Fig. 2
β_s, δ_s	= store yaw and pitch angle, respectively
γ_j	= singularity strength
$\tilde{\omega}_{ij}$	= velocity influence coefficient
ω_j	= velocity component at flow grid point i
<i>Superscripts</i>	
a	= aircraft
s	= store

Introduction

THE computer code USTORE, developed to predict the separation behavior of external stores released from aircraft, is discussed. The aircraft is represented by singularity panels in the same manner as in Woodward's USSAERO code.¹ The various versions of the USSAERO code, including some with external flowfield and external store capability,² suffer from a basic error in the perturbation velocity calculation which would make the calculation of external store loads incorrect in cases where the aircraft has tapered wings.³ This observation, at the time, was the starting point for the development of USTORE. The mathematical analysis

underlying USSAERO was thoroughly checked and resulted in a new computer code in which the errors of USSAERO were absent. This new code was fitted with external flowfield, external store, and store separation capabilities to become the USTORE code.^{4,5} In order to treat external stores of arbitrary geometry, the stores are also represented by singularity panels, in the same manner as the aircraft. Computer times per trajectory are reduced drastically by employing a flow grid method in combination with approximations regarding the aircraft-store interaction.

The separation predictions compare favorably with those obtained with the Nielsen-Goodwin-Dillenius separation code which is faster but restricted to stores of simple geometry due to the simplified approach employed to calculate the store loads. The results also indicate that lower-order panel methods, such as USSAERO and USTORE, can be quite valuable in store separation studies, in spite of the efforts directed at higher-order panel methods in this regard.⁶

The Panel Method

The basic philosophy behind USTORE, insofar as the panel method concepts are concerned, is the same as used in Woodward's USSAERO code,¹ and is therefore only outlined briefly.

The method is based on linear potential flow theory along the following lines. The surface of the aircraft and external store is subdivided into a large number of panels, each of which contains an aerodynamic singularity distribution. Constant source distributions are used on the panels of body components. Linearly varying vortex distributions are used on the panels of lifting surfaces to represent lift effects due to incidence, camber, and twist. The thickness of lifting surfaces is represented by linearly varying source distributions on their panels (the planar boundary condition option is used only). A control point is associated with each panel. The three perturbation velocity components, induced by each of the singularities, are calculated at the control points, and from these the components normal to the panels are formed. The magnitude of the normal velocity component induced in control point i by the singularity j of unit strength is called the aerodynamic influence coefficient a_{ij} . The resultant normal velocity component at control point i is then given by summation of the products of the influence coefficients a_{ij} and the strengths of the singularities j . In this way a system of linear equations with coefficients a_{ij} is obtained, relating the magnitude of the normal velocities at the control points to the

Received March 16, 1983; revision received Dec. 5, 1983. Copyright © American Institute of Aeronautics and Astronautics, Inc., 1984. All rights reserved.

*Head, Computational Aerodynamics Section, Aeronautics Department.

unknown singularity strengths. The singularity strengths that satisfy the boundary condition of tangential flow at the control points for a given Mach number and angle of attack are determined by solving this system of equations using an iterative procedure. Once the singularity strengths are known, the pressure coefficients at the control points are calculated in terms of the local perturbation velocity components. The forces and moments acting on the configuration, including the loads on external stores, are obtained by numerical integration of these pressures. Also, the perturbation flowfield created by the singularities of a configuration is readily obtained once the singularity strengths are known.

The method has been developed for both subsonic and supersonic flight conditions. Compressibility effects are taken into account by means of a Goethert-type rule. Viscosity effects are excluded (inviscid flow).

A typical example of the generally good results obtained with this approach is given in Fig. 1. This figure presents the longitudinal aerodynamic characteristics for an aft tail fighter configuration in subsonic and supersonic freestream flow. The wing has camber and twist and the horizontal tail is deflectable. Data are shown for two horizontal tail settings and for the case where the horizontal tail is absent. This case was, inter alia, run with 96 body panels and 110 lifting surface panels per symmetry half. Many comparisons between USTORE and experimental data have been compiled in Ref. 5.

The Aircraft-Store Interaction

USTORE has a multiple store position option with which the store loads for a set of various store positions (and orientations) can be computed in one run. Such a situation occurs, for example, in store separation calculations. In order to reduce the computer times to acceptable levels, USTORE was fitted with the "flow grid option." In this option, the isolated store moves through the nonuniform flowfield consisting of the freestream plus the perturbation field created by the aircraft. The nonuniform flowfield is defined at the mesh points of a three-dimensional orthogonal grid covering the separation region of interest. The grid is aligned with the aircraft coordinate system. The presence of the store has no direct influence on the perturbation flowfield but its effect on the flowfield enters through the values of the aircraft singularity strengths as follows.

A parameter I_{approx} has been introduced which can be assigned the value 1, 2, or 3 in the input data. These values represent different approximations.

In the option $I_{\text{approx}} = 1$, the aircraft singularity strengths are determined for the aircraft in isolation and remain constant. This is equivalent to assuming that the store is sufficiently small with respect to the aircraft that its influence on the aircraft can be neglected. The option $I_{\text{approx}} = 1$ will give deviations from the store loads calculated in the exact manner, but these deviations will decrease as the store gets further away from the aircraft. Let the body source and wing vortex singularity strengths γ_j^a of the aircraft in this option be denoted by subscript 1, viz $(\gamma_j^a)_1$.

In the option $I_{\text{approx}} = 2$, the aircraft singularity strengths are determined with the store in the release position (taking the full interaction between aircraft and store into account) and they remain constant irrespective of any subsequent store displacement. The store loads then will be well approximated in positions near the release position, the loads being exact in the release position. Let the body source and wing vortex singularity strengths γ_j^a of the aircraft in this option be denoted by subscript 2, viz $(\gamma_j^a)_2$.

In the option $I_{\text{approx}} = 3$, the body source and wing vortex singularity strengths γ_j^a of the aircraft are assumed to be a

† This means that the full matrix equation for aircraft and store is solved simultaneously at each store position, so that full mutual interaction between aircraft and store always is taken into account.

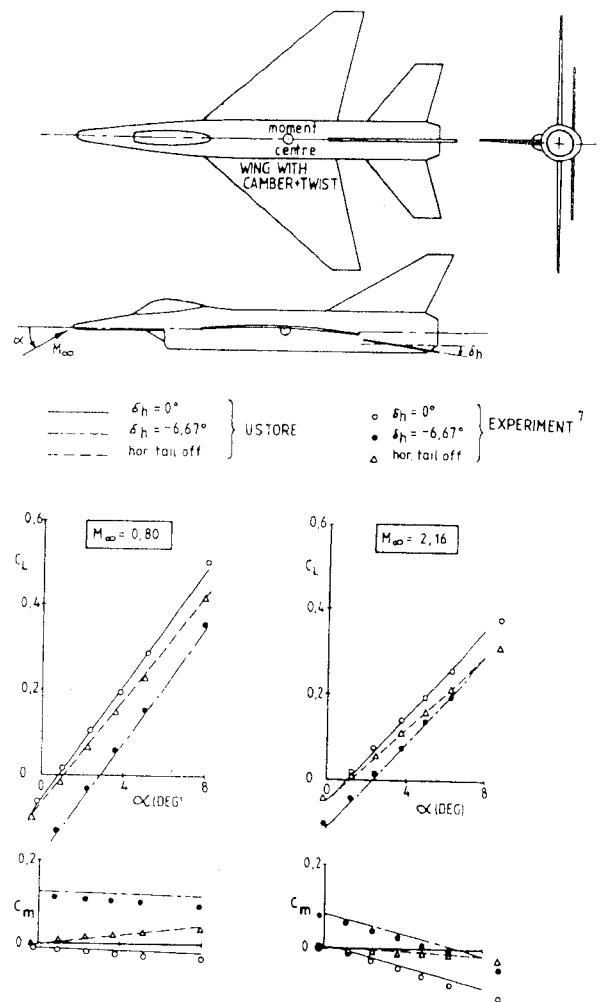


Fig. 1 Longitudinal characteristics of fighter configuration at subsonic and supersonic speeds.

function of $(\gamma_j^a)_1$ and $(\gamma_j^a)_2$ and the position of the store below the aircraft. A suitable function must be devised that gives store loads close to the exact store loads for any vertical store position. As a first attempt a linear function of the form

$$\gamma_j^a = \frac{Z_0}{Z} (\gamma_j^a)_2 + \left(1 - \frac{Z_0}{Z}\right) (\gamma_j^a)_1 \quad (1)$$

was used. Here Z and Z_0 denote the vertical distance of the store from the aircraft in an arbitrary store position and release position, respectively. In the release position $Z_0/Z = 1$ and the exact store loads are then obtained. At further distances away from the aircraft the store loads should again match the exact store loads closely, as the ratio Z_0/Z becomes increasingly smaller.

Let $\bar{\omega}_{ij}$ be any of the velocity components (u, v, w) induced at grid point i by aircraft singularity j of unit strength; $\bar{\omega}_{ij}$ is called a velocity influence coefficient. These velocity influence coefficients at the grid points need to be calculated only once and then can be used for any subsequent store position and orientation and for any angle of attack of the aircraft (if keeping the freestream Mach number constant). The resultant perturbation velocity component ω_i at grid point i generated by the aircraft is then given by summation of the products of the velocity influence coefficients $\bar{\omega}_{ij}$ and the strengths γ_j^a of the aircraft singularities j , viz,

$$\omega_i = \sum_{j=1}^{N^a} \bar{\omega}_{ij} \gamma_j^a \quad (2)$$

Here N^a denotes the total number of aircraft singularities, viz, the body source and wing vortex singularities (whose strengths γ_j^a are obtained in accordance with the I_{approx} option selected) and the wing source singularities (whose strengths γ_j^a are constant and a function of the local wing thickness slope only). The α dependence of the perturbation flowfield comes through the α dependence of the body source and wing vortex strengths γ_j^a of the aircraft.

Summarizing, in the option $I_{\text{approx}} = 1$ the flowfield below the aircraft is completely unaffected by the store presence. In the options $I_{\text{approx}} = 2, 3$ there is an indirect influence of the store on the flowfield. If $I_{\text{approx}} = 2$, this influence is exactly correct only if the store is in its release position; the flowfield remains unchanged for subsequent store positions. In option $I_{\text{approx}} = 3$, the flowfield changes when the vertical position of the store is changed [in accordance with Eq. (1)]. The store now moves through this aircraft flowfield in isolation.

The aircraft perturbation flowfield velocities at the store control points are obtained by interpolation from the velocity components at the grid points and then are incorporated into the boundary condition of tangential flow at the store control points. These store boundary conditions also include the motion of the store. This results in the usual manner in a system of linear equations for the store

$$\sum_{i=1}^{N^s} \sum_{j=1}^{N^s} a_{ij}^s \gamma_j^s = - \sum_{i=1}^{N^s} (n_{\infty i}^s + n_{p_i}^s + n_{t_i}^s + n_{f_i}^s) \quad (3)$$

Here $n_{\infty i}^s$ is the normal component of the freestream velocity vector at store control point i , $n_{p_i}^s$ is the normal component at store control point i of the aircraft perturbation flowfield defined at the flow grid, $n_{t_i}^s$ is the constant normal velocity induced at store control point i by the store wing source distributions (of constant and known strengths), and $n_{f_i}^s$ is the normal component of the velocity at store control point i due to the translatory and angular motion of the store relative to the aircraft. N^s denotes the total number of store control points (equal to the total number of body source and wing vortex singularities γ_j^s of the store).

The right-hand members of Eq. (3) are known at each store position in the flow grid. In addition, the aerodynamic influence coefficients a_{ij}^s for the influence of store singularity j of unit strength on store control point i are constant and need not be recalculated at each store position. The calculations per store position are thus basically determined by the speed of the numerical method with which store matrix Eq. (3) is solved for the unknown body source and wing vortex singularity strengths γ_j^s of the store.

Once the store singularity strengths are known the store loads are calculated in the usual manner and applied in the equations of motion to obtain the separation characteristics.

The most attractive proposition in store separation trajectory calculations is the option $I_{\text{approx}} = 1$, because it opens the way to make use of a library of data files, which is continuously extended. As a matter of routine the matrix of aerodynamic influence coefficients a_{ij}^a of each new aircraft configuration is permanently stored on file as well as the velocity influence coefficients $\bar{\omega}_{ij}$ at the points of the corresponding flow grid. The same is done for existing configurations at a new freestream Mach number. This is done because a_{ij}^a and $\bar{\omega}_{ij}$ are independent of the aircraft angle of attack α but dependent on the freestream Mach number and the aircraft geometry. In the same manner the matrix of aerodynamic influence coefficients a_{ij}^s is filed for each new store configuration at each new freestream Mach number. In this way the library of data files is continuously extended. The ultimate objective is that, whenever new trajectory data are required, the matrix of aerodynamic influence coefficients a_{ij}^a for the particular aircraft and the flow grid data $\bar{\omega}_{ij}$ at the desired freestream Mach number are read from the corresponding files. The matrix equation for the aircraft is

then solved giving the aircraft singularity strengths γ_j^a at the desired aircraft angle of attack. From the coefficients $\bar{\omega}_{ij}$ the flowfield below the aircraft is then known at that particular α value, Eq. (2). In addition, the aerodynamic matrix for the store under consideration is read from the files. In this manner, all of the data that are required prior to the actual store trajectory calculations are obtained fast and efficiently. Without such a data library, the time-consuming calculation of the coefficients a_{ij}^a , $\bar{\omega}_{ij}$, and a_{ij}^s would have to be performed at each new run. The actual trajectory calculations themselves are quite economical, typically a couple of minutes per separation calculation; they are described in the next sections.

An additional advantage of the $I_{\text{approx}} = 1$ option is that at no stage need the spanwise paneling of the lifting surfaces of the store and the spanwise paneling of the lifting surfaces of the carrier aircraft be matched. In the options $I_{\text{approx}} = 2, 3$ this matching would be required if the store in carriage position is close to the wing (and pylon) of the aircraft. The $I_{\text{approx}} = 1$ option will therefore, in general, result in a saving in the number of aircraft wing (and pylon) panels in the region of the attached store and a saving in the number of store panels. The computer times are reduced accordingly.

If separation problems are apparent from the $I_{\text{approx}} = 1$ calculations, the situation can be checked using the $I_{\text{approx}} = 2$ or 3 option.

Store Separation

The separation characteristics of the released store are obtained as follows. First, USTORE calculates the forces and moments acting on the store in the release position. The program numerically integrates the six-degree-of-freedom equations of motion for the store for a specified small time interval Δt to arrive at a new store position and attitude in the flow grid. During this time interval the store forces and moments acting on the store in the release position. Then the acting on the store at its new position and attitude are computed and the equations of motion again solved for a small time interval. This procedure is repeated giving the time histories of the position and attitude of the store after its release in a quasisteady step-by-step manner. The numerical integration scheme uses Merson's form of the Runge-Kutta method (single step).

UNSTORE can simulate the actual (free-flight) store separation trajectories as well as captive-store trajectories.

The separation of the store from the carrier aircraft in the actual free-flight situation is accounted for in USTORE by incorporating the velocities at the store control points due to the translatory and angular motions of the store, into the boundary condition of tangential flow at the store control points. In this way aerodynamic damping is simulated.

In the next section USTORE will be compared with experimental captive-store separation trajectories. In the experimental captive-store technique the free-flight separation trajectory cannot be simulated exactly. If damping is to be

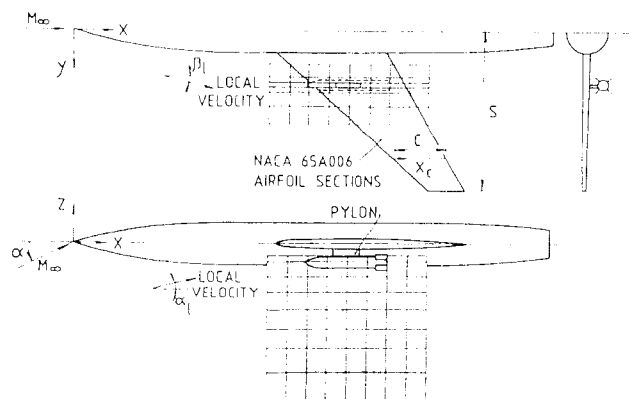


Fig. 2 Aircraft/external store configuration.

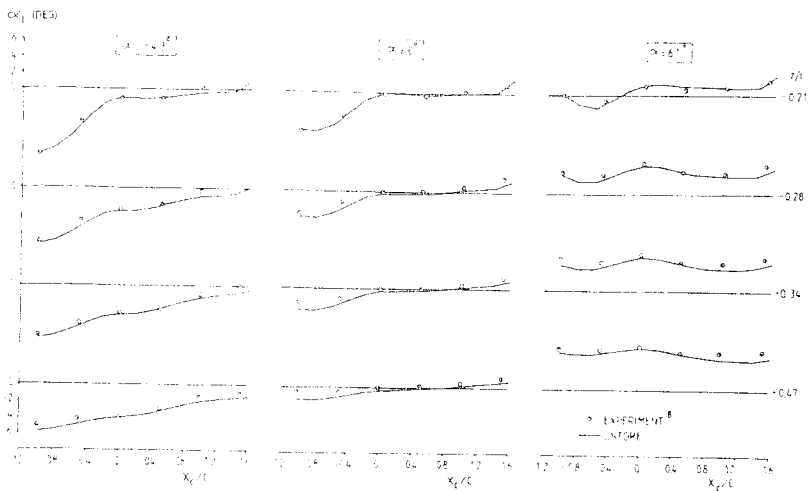


Fig. 3a Flowfield below isolated aircraft in incompressible flow; pylon is absent; vertical flow angularity at $y/s=0$.

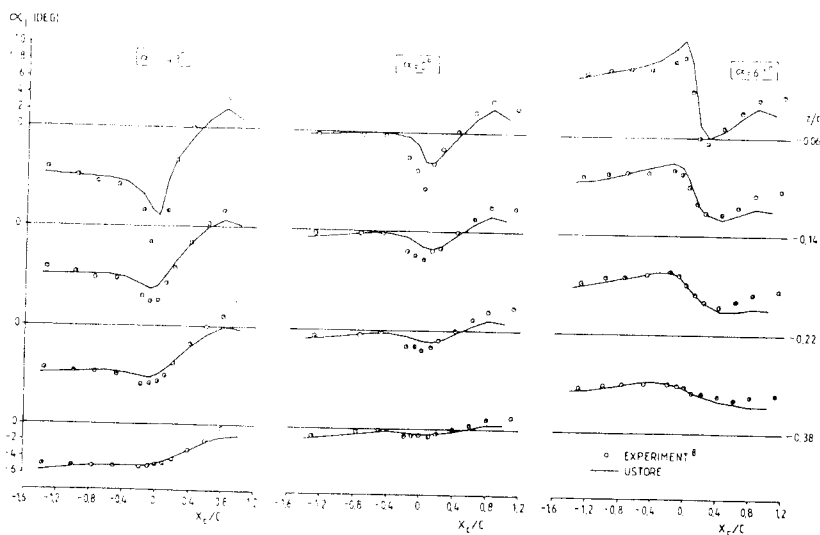


Fig. 3b Flowfield below isolated aircraft in incompressible flow; pylon is absent; vertical flow angularity at $y/s=0.25$.

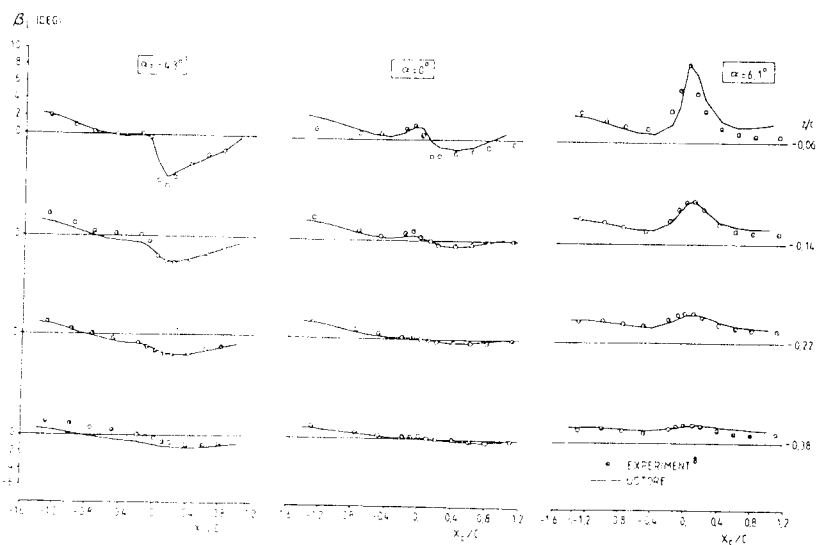


Fig. 3c Flowfield below isolated aircraft in incompressible flow; pylon is absent; lateral flow angularity at $y/s=0.25$.

included in the captive-store method, it must be fed into the problem by specifying damping coefficients. Also, in the experimental captive-store trajectories, the store yaw and pitch angles are changed geometrically in the wind tunnel during the measurement of the store loads to account for the incidence induced by the translational velocities of the store relative to the aircraft. This change in store attitude in the wind tunnel causes the store, in effect, to be in a different part of the interference flowfield. The captive-store technique just described also can be simulated by USTORE.

Results

Results obtained with USTORE will be presented for the aircraft/external store combination shown in Fig. 2. Apart from experimental data regarding aircraft flowfield and external store loads, experimental separation trajectory data also are available for this combination.

Figure 3 compares USTORE with experimental flowfield data below the isolated carrier aircraft. Axial distributions of the local flow angularities are presented for various angles of

attack, various distances below the aircraft, and various spanwise stations. The flow angularities α_f and β_f are defined in Fig. 2. The estimated experimental errors are ± 1.0 deg for the vertical flow angularity α_f and ± 1.5 deg for the lateral flow angularity β_f .⁸ The variations of the flow angularities are predicted satisfactorily by USTORE. The USTORE results were obtained with 126 body panels and 378 lifting surface panels per aircraft symmetry half.

The external store load and trajectory calculations were performed with a minimum number of store panels, viz, 8 panels per store fin and 36 store body panels. Figure 4 shows that so few panels still give satisfactory agreement with the experimental freestream characteristics for the store. The aircraft is represented by 64 body panels and 115 wing plus pylon panels per symmetry half.

The effect of I_{approx} on the external store loads is considered first and compared with the exact solution. In the options $I_{approx} = 2, 3$ it was found that the differences in the store forces and moments do not differ more than about 1% with respect to the exact solutions for store positions covering the whole vertical range from carriage position to infinitely far away from the aircraft. For $I_{approx} = 1$, the differences with respect to the exact solutions were larger but still can be considered quite small (see Fig. 5); the maximum differences occur in the carriage position as is to be expected. For the configuration under consideration, the influence of the store on the aircraft apparently may be neglected in calculating the loads on the external store. As a matter of fact, it is expected that this is the case for the vast majority of aircraft/external store configurations.

The effect of the aircraft angle of attack on the store loads is shown in Fig. 6. The experimental data were obtained from Ref. 9, which showed large fluctuations of experimental store loads in the carriage position. For this reason the store has been taken 1.5 store diameters below the carriage position. At this position the fluctuations in the experimental data are sufficiently small to allow a comparison with USTORE. It

should be noted that in this position the interference effects of the aircraft on the store loads are still very pronounced, as is seen readily by comparing Fig. 6 with Fig. 4. The USTORE results are obtained with the option $I_{approx} = 1$. In Ref. 5, a strong case is made that the differences between the experimental forces and moments on the store and the USTORE results are accounted for by the differences in the experimental and calculated perturbation flowfield velocities.

The experimental captive-store trajectory data presented in this section are obtained using the technique described in the previous section. No damping was fed into the problem. This captive-store technique was simulated by running USTORE in the corresponding trajectory option.

All USTORE trajectories have been obtained using the flow grid option in the $I_{approx} = 1$ mode and a time step $\Delta t = 0.02$ s. Initially (at time $t = 0$), the ejected store is one store radius below the attached position on the pylon. At that time the store longitudinal axis is parallel to the longitudinal axis of the aircraft fuselage and the store has a 45-deg roll attitude. The initial values of the angular velocity components of the store are zero. The (downward) ejection velocity of the store is 3 m/s (relative to the aircraft). The mass of the store is 227 kg, its axial and transverse moments of inertia are 11 and 110 kg-m², respectively, and the center of mass is located at the store midpoint. It should be mentioned that the above data represent full-scale conditions. The flight conditions vary in that two aircraft angles of attack ($\alpha = 0$ and 6 deg) and two freestream Mach numbers ($M_\infty = 0.4$ and 0.7) are considered. The aircraft is in level flight (zero climb or dive angle) at an altitude of 1525 m.

The calculated and experimental store separation characteristics are presented in Figs. 7a and 7b for the angular motion of the store and the center of mass motion relative to the aircraft. The flow grid used in the USTORE calculations is

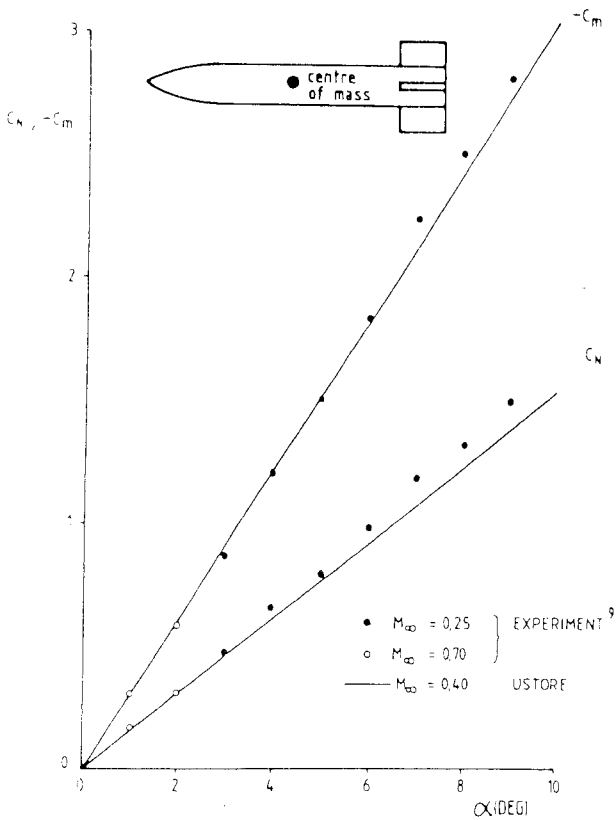


Fig. 4 Aerodynamic data for the isolated external store at 45 deg roll attitude.

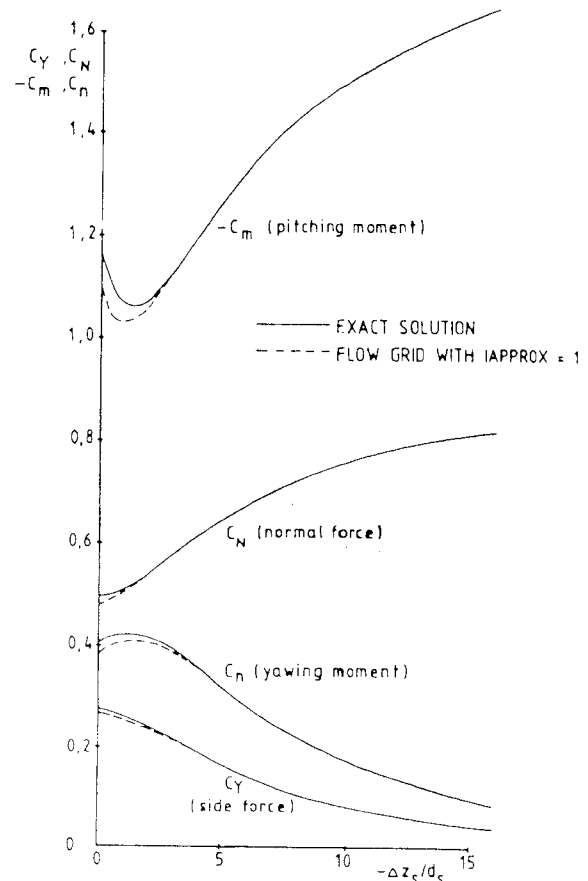


Fig. 5 Calculated external store loads as a function of the vertical distance from the carriage position; pylon is absent; $M_\infty = 0.4$, $\alpha = 6$ deg.

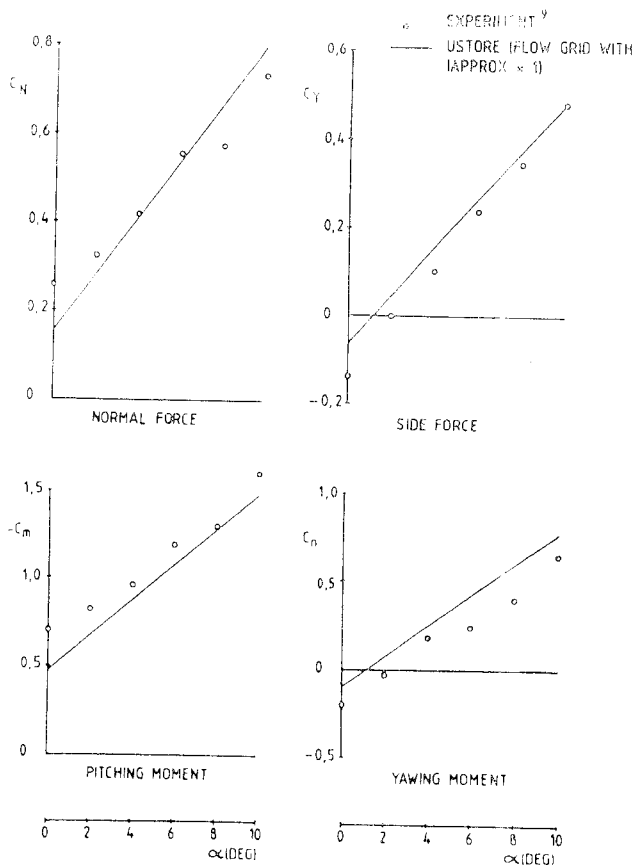
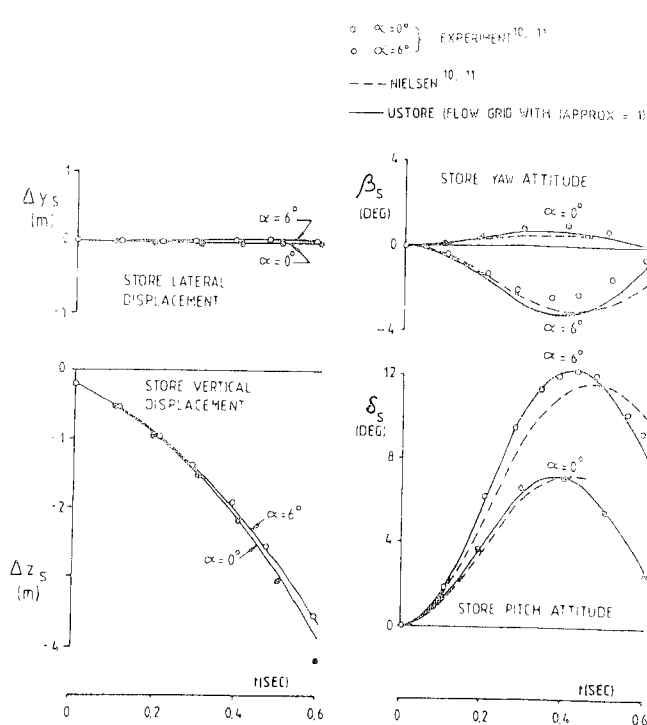


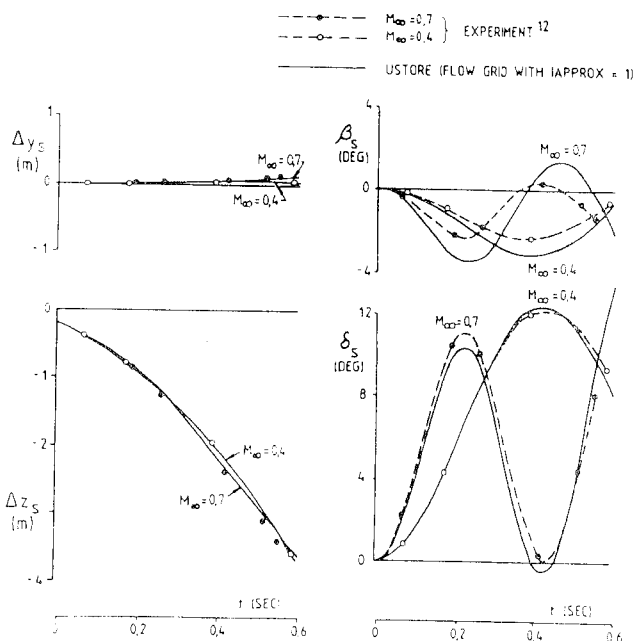
Fig. 6 Variation of external store loads with aircraft angle of attack; store is 1.5 store diameters below carriage position; pylon is present; store has a 45 deg roll attitude; $M_\infty = 0.25$.

shown in Fig. 2. Figure 7a presents the effect of the aircraft angle of attack on the store separation. The predictions by both Nielsen and USTORE are shown for the yaw and pitch histories of the store. The Nielsen data for the displacements of the store's center of mass are not shown since they are very close to the displacements calculated by USTORE. Both methods, but in particular USTORE, provide quite satisfactory predictions of the behavior of the store after release. Figure 7b shows the experimental and calculated effects of the aircraft flight velocity (Mach number). The lateral displacements of the store's center of mass are very small, even for the high Mach number case. Unfortunately, no Nielsen trajectory data were available for the conditions represented in Fig. 7b. The agreement between USTORE and the experimental separation characteristics is satisfactory. The largest differences occur in the store yaw histories. It should be mentioned that the uncertainties in the experimental trajectory data can be substantial. Reference 12 gives the estimated maximum uncertainties in the experimental store yaw angle β_s 0.5 s after release as ± 1.0 deg (at $M_\infty = 0.4$) and ± 1.9 deg (at $M_\infty = 0.7$).

Each of the above trajectories calculated with USTORE required less than 3 min of CPU time on a CDC Cyber 174 computer. This excludes the time required to calculate the aerodynamic matrix of the aircraft/store combination and the velocity influence coefficients at the flow grid points prior to the actual trajectory calculations. The time required to calculate these data depends basically on the number of panels and the number of flow grid points; in the present case it takes about 15 min of CPU time. These data are independent of such parameters as the aircraft angle of attack, dive (or climb) angle, flight altitude, store mass properties, and initial conditions of the store. It is thus possible to calculate a set of trajectories in one run, each representing a different combination of the abovementioned parameters, without needing



a) Effect of aircraft angle of attack α ; $M_\infty = 0.4$.



b) Effect of freestream Mach number M_∞ ; $\alpha = 6$ deg.

Fig. 7 Captive-store separation trajectories; pylon is present; no damping.

to recompute the aerodynamic matrix and flow grid velocity influence coefficients at the start of each new trajectory. As explained earlier, there is also the opportunity to extract such data from a library of data files, which would remove altogether in a variety of cases the computation of the aerodynamic matrix and flow grid velocity influence coefficients.

In order to assess the importance of damping on the motion of the store, the trajectory for a particular case also was calculated with damping included in all three angular motions. The USTORE results showed that the effect of damping was negligible except in the pitching oscillation

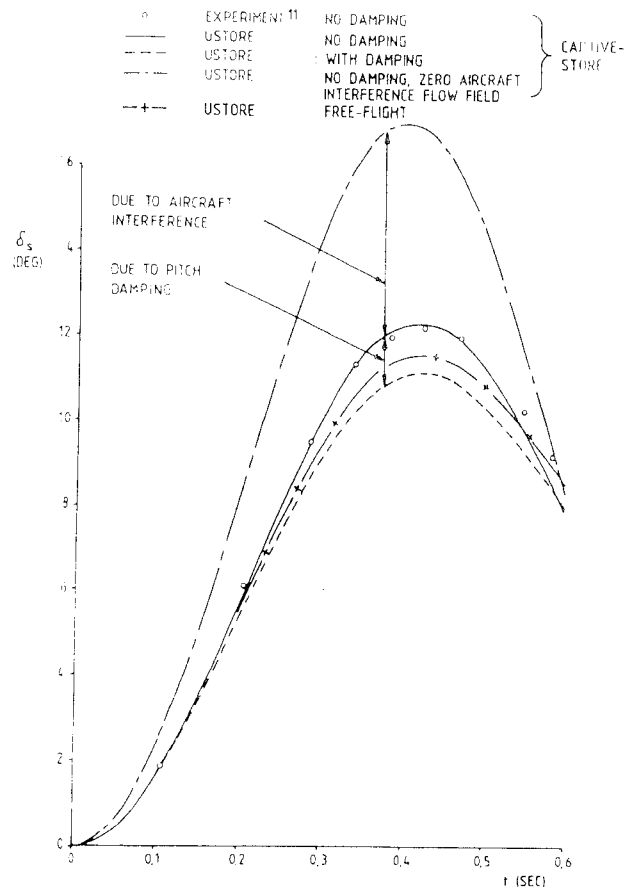


Fig. 8 Calculated influence of pitch damping and aircraft interference flowfield; $M_\infty = 0.4$ and $\alpha = 6$ deg.

which was reduced in maximum amplitude by about 1 deg as the result of pitch damping, see Fig. 8. Another theoretical curve also has been added to Fig. 8. This curve is the pitch angle history when there is no aircraft interference flowfield. The effect of the interference flowfield is significant and is well predicted by USTORE. Also included is the calculated pitch motion under real free-flight conditions. As expected, the differences with the captive-store trajectory results with damping included are small.

More examples of store separation predictions with USTORE are given in Ref. 5, including an unsafe release prediction in supersonic flight conditions.

References

- Woodward, F. A., "An Improved Method for the Aerodynamic Analysis of Wing-Body-Tail Configurations in Subsonic and Supersonic Flow. Part I—Theory and Application," NASA CR-2228, May 1973.
- Woodward, F. A., "USSAERO Computer Program Development, Versions B and C," NASA CR 3227, April 1980.
- van den Broek, G. J., "Correction to the Wing Source Velocity Error in Woodward's USSAERO Code," *Journal of Aircraft*, Vol. 20, July 1983, pp. 628-632.
- van den Broek, G. J., "The Analytical Prediction of the Separation Behaviour of External Stores after Release from the Carrier Aircraft. Part I—Theory," National Institute for Aeronautics and Systems Technology, Pretoria, South Africa, NIAST Rept. 79/103, Sept. 1980.
- van den Broek, G. J., "The Analytical Prediction of the Separation Behavior of External Stores after Release from the Carrier Aircraft. Part II—Applications," National Institute for Aeronautics and Systems Technology, Pretoria, South Africa, NIAST Rept. 79/103, Aug. 1979.
- Čenko, A., Tinoco, E. N., Dyer, R. D., and DeJongh, J., "PAN AIR Applications to Weapons Carriage and Separation," *Journal of Aircraft*, Vol. 18, Feb. 1981, pp. 128-134.
- Dollyhigh, S. M., "Subsonic and Supersonic Longitudinal Stability and Control Characteristics of an Aft Tail Fighter Configuration with Cambered and Uncambered Wings and Uncambered Fuselage," NASA TM X-3078, Aug. 1974.
- Alford, W. J. and King, T. J., "Experimental Investigation of Flow Fields at Zero Sideslip Near Swept- and Unswept-Wing-Fuselage Combinations at Low Speed," NACA RM L56J19, 1957.
- Bergrun, N. R. and Goodwin, F. K., "Data Report for the External Stores Test Program. Volume II—First Tunnel Entry Force and Moment Data," Nielsen Engineering and Research, Inc., Mountain View, Calif., NEAR Rept. TR 24, Vol. II, Oct. 1970.
- Goodwin, F. K., Dillenius, M.F.E., and Nielsen, J. N., "Method of Predicting Loading and Trajectories of Single or TER or MER Mounted Stores on Swept-Wing Aircraft," AFFDL-TR-72-67, Vol. 2, Aug. 1972.
- Dillenius, M.F.E., Goodwin, F. K., and Nielsen, J. N., "Extension of the Method for Predicting Six-Degree-of-Freedom Store Separation Trajectories at Speeds up to the Critical Speed to Include a Fuselage with Noncircular Cross Section. Volume I—Theoretical Methods and Comparisons with Experiment," AFFDL-TR-74-130, Vol. 1, Nov. 1974.
- Roberts, R. H. and Myers, J. R., "Flow-Field Characteristics and Aerodynamic Loads on External Stores Near the Fuselage and Wing-Pylon Positions of a Swept-Wing/Fuselage Model at Mach Numbers of 0.4 and 0.7—Phase V," Arnold Engineering Development Center, AEDC-TR-73-87, March 1974.